Molecular insight into the Mullins effect: Irreversible disentanglement of polymer chains revealed by molecular dynamics simulation

Chi Ma[1], Tuo Ji[2], Christopher G. Robertson[3], R. Rajeshbabu[4], Jiahua Zhu[2], and Yalin Dong[1]*

1. Department of Mechanical Engineering, The University of Akron, Akron, OH, 44325, USA
2. Intelligent Composites Laboratory, Department of Chemical and Biomolecular Engineering, The University of Akron, Akron, OH, 44325, USA
3. Cooper Tire & Rubber Company, 701 Lima Ave, Findlay OH 45840, USA
4. Apollo Tyres Ltd, Oragadam, Sriperumbudur 602105, Tamilnadu, India

Email: ydong@uakron.edu

Abstract

The debate on the possible molecular origins of the Mullins effect has never ceased since its discovery. To tackle this issue, Molecular dynamics (MD) simulation is carried out to elucidate the underlying mechanism of the Mullins effect. For the first time, the key characteristics associated with the Mullins effect including (a) the majority of stress softening occurring in the first stretch, (b) continuous softening with stress increase, (c) permanent set, and (d) recovery with heat treatment, are captured by molecular modeling, laying out a solid foundation to use MD simulation to study the Mullins effect. It is discovered that the irreversible disentanglement of polymer chains is physically sufficient to interpret these key characteristics, providing molecular evidence for the long-controversial issue. Our results also reveal that filled rubber exhibits three distinct regimes in terms of stiffness, i.e., polymer matrix, interface, and filler. When subjected to external strain, polymer matrix suffers from excess deformation, indicating strong heterogeneity within filled rubber. The new understanding would provide molecular insight for the formulation of physically based constitutive relations for filled rubber.

Introduction

When subjected to stretch, rubber-like materials experience substantial stress softening. As shown in Figure 1, the so-called Mullins effect, observed in a wide range of materials from rubber [1–6], polymer gels [7,8], and living tissues [9,10], exhibit a few key characteristics. (1). The first stretch accounts for the majority of stress softening and the consecutive cycles of stretch with equal or less strain afterwards do not soften the material substantially. (2). Permanent set (residual strain) is left after the first stretch. (3). The so-called permanent set is indeed not permanent, can partially or even fully recover when exposed to high temperature. (4). When the stretch exceeds the maximum strain of previous stretches, the stress-strain curve returns to the monotonous uniaxial stretch route. It is worth mentioning that, while the majority of the studies of the Mullins effect focus on filled rubber, stress softening is also observed in unfilled nature rubber when it is stretched to the same tress level (instead of strain) as its filled counterpart [1,11], indicating a universal principle lying in these distinct systems.

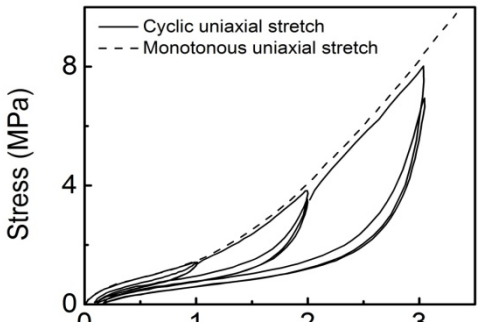

Figure 1 The typical stress-strain curve of carbon black filled SBR adopted from [15].

Although the Mullins effect has been discovered for more than one century by Bouasse and Carriere [12], and has been intensively studied for more than six decades thanks to Mullins' seminal work [2,6,11,13], the molecular mechanism underlying the Mullins effect remains controversial [14,15]. The controversy lies in the technical challenge of *in situ* "seeing" microstructure change at the nano-scale during mechanical stretching of rubber, as well as the complexity of rubber system as a mixture of fillers, polymer matrix and filler/polymer interfaces. Up to date, a number of physical interpretations have been proposed and can be approximately grouped into three categories [16], namely, (1) irreversible processes within polymer matrix: cavity formation, chain scission, disentanglement, and crosslink breakage; (2) irreversible processes within filler network: filler aggregate or agglomerate fracture, and rupture of the carbon-black network (loss of percolation); (3) irreversible processes at polymer-filler interface: molecule slips, molecule adsorption, and bond breakage at the filler surface. The lack of a well-established physical interpretation hinders the development of physics-based constitutive laws for mechanical behaviors of rubber-like materials. With the wide usage of finite element modeling in rubber industry, there are a lot of efforts to formulate constitutive equations to describe non-linear superplastic, and time-dependent viscoelastic behaviors of rubber-like materials [17–23]. Particularly, a lot of endeavors have been made to capture the stress-softening phenomenon, and most of the current models are phenomenological based [17,19,20]. Even though they can be easily adopted in finite element analysis packages and proved effective for some materials under certain conditions, these phenomenological constitutive laws cannot be generalized and fall short in many applications [17,19]. Physics-based constitutive laws have also been proposed to address these issues. However, they are plagued by the lack of fundamental understanding of underlying mechanisms. As a result, their parameters which are supposed to relate to the claimed physics, when fitted, fail to agree with experimentally measured physical parameters [15]. There is an urgent need to gain a molecular insight into the Mullins effect.

Although a direct observation of molecular level evolution during rubber stretching is tremendously challenging for experimentalists, numerous works have been conducted to have indirect characterizations. We summarize the key and consensus experimental observations, which can serve as established guidelines to validate our molecular modeling. Swelling test can be used to characterize the density of crosslink in rubber. Experimental results from swelling tests by different research groups show that there is no significant crosslink or chain break after stretching, implying the damage to polymer matrix (chain break or crosslink break) is not ready to explain the Mullins effect [16,24]. When using carbon black as fillers, filled rubber can acquire electrical conductivity. The rupture of filler structure affects the electrical conductivity of filled rubber, which can thus serve as an indicator for filler breakage. In [16], along with stress softening the rupture of filler cluster was detected by measuring electrical conductivity. However, while the Mullins effect was recovered when subjected to elevated temperature the filler structure was not, indicating the filler network alteration is not the vital factor for stress softening. It is also noted that the Mullins effect is observed in a wide range of materials including unfilled rubber and living tissues, which cannot be explained by the conjecture based on filler/polymer interface change. If a proposed mechanism is a general principle, it should comply with existing experimental observations.

Molecular dynamics (MD) simulation is a powerful tool to "see" the micro structural evolution *in situ* within rubber when subjected to stress. With the advent of supercomputer, MD is being used to explore molecular origins for mechanical behaviors of polymer-based materials [25–35]. While most MD research investigates mechanical reinforcement, few works focus on stress softening. As a matter of fact, if the most fundamental behavior could not be captured by MD simulation, it hurts the credibility of MD simulation in elucidating molecular origins of mechanical properties of filled rubber. In this study, by developing a MD simulation of a filled polymer system, to the best of our knowledge, it is the first time that the key characteristics of the Mullins effect (stress softening, permanent set, recovery, continuing softening with

strain increase) are captured. Equipped with the model, we will have a systematic study of molecular origins of the Mullins effect. We will also interrogate the revealed molecular mechanism by comparing with available experimental observations.

Methodology

The targeted system is styrene-butadiene-rubber (SBR) reinforced with functionalized silica particles, a rubber material widely used in tire industry. A coarse-grained (CG) model is developed to simulate the filler/polymer nanocomposite system. The three basic elements of the system are elastomer, filler, and silane which bridges filler particle and elastomer chain. The procedure to build up the system is discussed below. Dimensionless unit is used in the simulation. To correlate CG model with an actual material (SBR), three basic units, mass unit m_0, energy unit ε_0, and length unit σ_0 are set as 282g/mol, 30 kj/mol and 2 nm separately [36]. All other units can be derived based on these three basic units.

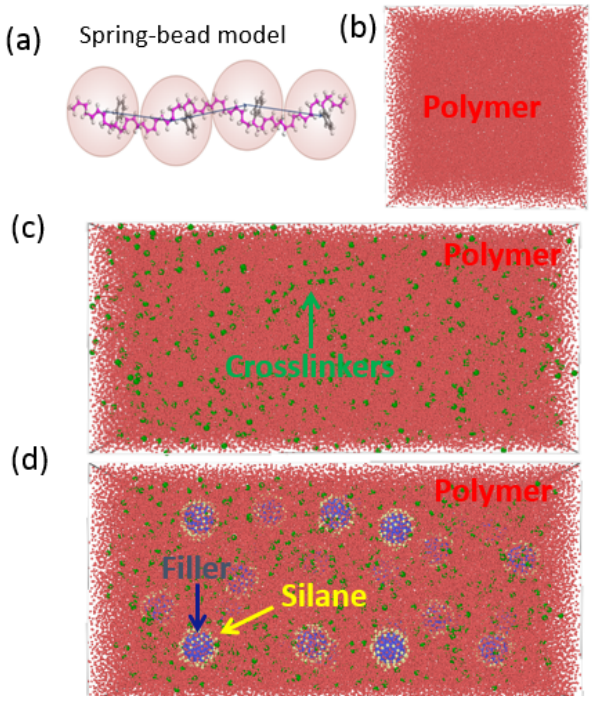

Figure 2 Molecular model for filled polymer system. (a). Spring-bead model. (b). Polymer matrix. (c). Crosslinked polymer matrix. (d). Filled polymer with grafted silane.

The first step is to build a polymer matrix. In the CG model, an elastomer is modeled as a bead-spring chain. As shown in Figure 2 (a), a bead is used to represent one repeating unit (also called monomer) with mass $m = m_0$. Random walk method is utilized to fill the space with elastomers. First, the head monomer is generated randomly in the simulation box. Following that, an adjacent monomer is generated and chemically bonded to the head monomer by abiding the two rules: the two monomers are in force balance position and there is no overlap between the new monomer and other existing monomers. Repeating this process, an elastomer with pre-defined number of bead and stochastic arrangement will be produced. Eventually, the simulation box is filled with elastomers and form a polymer matrix. The polymer matrix used in our simulation contains 300 elastomer chains and each elastomer chain has 400 beads. The system is thus exposed to isothermal-isobaric (NPT) process with $P^* = 0$ and $T^* = 1.5$ until there is no noticeable size and pressure variation, an indicator for thermodynamic equilibrium.

The second step is vulcanization, using Sulphur (S) atoms to crosslink elastomers. Vulcanization is a routine technique in polymer industry to increase mechanical strength. To add a Sulphur atom, we first randomly choose a point in the simulation box. We then search two monomers with the shortest and second shortest distances to the point and crosslink the two monomers with a S-S chemical bonding. By controlling the number of points, we can control the crosslink density of the system. The effect of crosslink density on mechanical performance studied by molecular dynamics can be found in one of our works [36]. In this study, 0.9% (weight fraction) sulfur is used in our simulation. Note that the bonding length ranges from S1 (one Sulphur) to S8 (eight Sulphurs) in reality, while in our simulation only S8 is used for simplification. After vulcanization, an NPT procedure is applied to relax the system as shown in Figure 2(c).

The third step is to embed functionalized fillers into polymer matrix. A filler takes a spherical shape and is composed of silica atoms. Its atomic structure allows silane molecules to be chemically grafted to its surface.

The diameter of filler is $d_f = 10\sigma_0 5$, and the mass of filler is 300 m_0, 300 times of monomer mass. To embed fillers into polymer matrix, points within polymer matrix are randomly chosen and virtual atoms with strong repulsive force are placed on these points to acquire spaces for fillers. The fillers grafted with silanes (grafting density 0.155 nm^{-2}) are then inserted to replace virtual atoms. After reaching equilibrium through NPT, a chemical bond will be manually introduced between silane and its nearest polymer monomer. In this way, fillers will be chemically connected with surrounding elastomers. Before having mechanical test, the system is once again exposed to NPT to reach equilibrium. The dimension of the relaxed system is 168 x 84 x 84 nm as shown in Figure 2(d).

To conduct mechanical tensile and compressive tests, we fix one end of the filled rubber, and stretch the other end with constant speed (corresponding a strain rate 4 x $10^8 s^{-1}$) for loading and the same constant speed when unloading. During stretching, NVT ensemble with $T^* = 1$ will be used. When each loading or unloading is accomplished, NVT equilibrium will be continuously imposed to the system for 3.2 x 10^5 time steps (2.0 ns physical time). During dynamic tests, free boundary conditions are applied in all directions. It is noted that the way we used to stretch the system is different from the way to uniformly deform the simulation box in most previous MD simulations. Our method allows all possible chain movements, which are essential for the Mullins effect.

There are two kinds of interaction, van der Waals force and covalent bonding force, which are represented by Lennard-Jones (L-J) potential and harmonic potential respectively in our simulation. When there is no chemical bonding, L-J potential as shown below is used,

$$E = 4\varepsilon\left[\left(\frac{\sigma}{r}\right)^{12} - \left(\frac{\sigma}{r}\right)^{6}\right] \quad r < r_c$$

where r_c is cutoff distance, σ and ε are pre-defined distance and energy parameters. The L-J parameters used for different materials are listed in Table 1.

TABLE 1: Parameters of L-J potential

	monomer-monomer	silane-silane	Filler-silane	silane-monomer	filler-monomer
ε (ε_0)	1.0	1.0	0.4	1.0	0.4
σ (σ_0)	1.0	1.0	1.0	1.0	1.0
$r_c(r_0)$	2.24	2.24	2.24	2.24	2.24

Covalent bond is modeled using a harmonic potential superposed with an L-J potential. The potential thus becomes,

$$E = K(r - r_0')^2 + 4\varepsilon\left[\left(\frac{\sigma}{r}\right)^{12} - \left(\frac{\sigma}{r}\right)^{6}\right]$$

where $r_0' = 0.98\, r_0$ and stiffness $K = 34$. The same parameters of harmonic potential are used for all chemical bonding including monomer-monomer, silane-monomer and silane-filler. Considering the much larger mechanical strength of fillers (silica) compared with polymer matrix, fillers are simplified as rigid bodies so that the interaction of atoms within filler can be neglected, which will substantially improve the computational efficiency.

Results

In this section, MD simulation is carried out to regenerate the key characteristics of the Mullins effect, i.e., permanent set, stress softening during the first stretch, recovery of the Mullins effect at elevated temperature, and continuing softening with strain increase. After reproducing the experimental observations, microstructure analysis will be conducted to unveil their molecular origins.

The first observation is permanent set. The filled rubber is stretched to strain up to 300%, and then released back to the state with zero stress response. From Figure 3(a), we can see, when released, the filled rubber cannot recover to its original shape. Instead, a residual strain is left. By fitting the releasing stress strain curve with a second-order polynomial, the residual strain is determined. With the strain of 300%, the residual strain is 79%. The inability to return to its original shape is called permanent set, and is routinely observed in experiments. Indeed, in Mullins' seminal work, permanent set has been observed in both pure nature rubber and filled nature rubber [37]. To compare with experiments, we list some values of residual strain reported in literature. Dorfmann and his co-works reported residual strain ranging from 0-20% for carbon black filled nature rubber for different filler densities and maximum strains [38]. It was also found that residual strain increases with applied maximum strain, which is consistent with our simulation. We observe the increase of residual strain from 53% to 79% when the maximum strain from 100% to 300% as shown in Figure 3(b) In Diani's work, a residual strain of 31% was observed by stretching a filled EPDM to 200%. It is noticed that the residual strain obtained in our simulation is larger than those observed in experiments. We attribute the value difference to the strain rate gap between simulation and experiment. The residual strain is known to be related to many factors including material, filler density, stretching strain, strain rate, and temperature [38–40]. In our simulation we are able to match most parameters; however, the strain rate used in the simulation is orders of magnitude larger than that used in experiment measurement. In our simulation, a super-high strain rate 4 x $10^8 s^{-1}$ is applied due to computational limitation. This super-high strain rate gives less time for the system to recover, as a result, a larger residual strain.

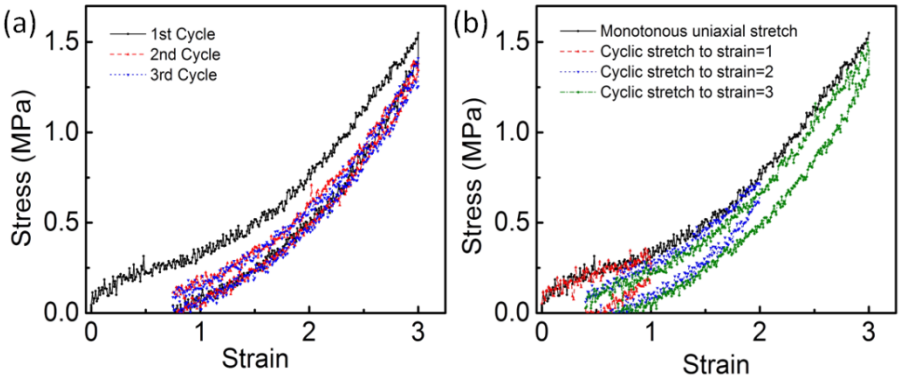

Figure 3 Stress-strain curves of filled rubber. (a). Stress-strain curves for different cycles. (b). Stress-strain curves by increasing maximum strain from 1, 2 to 3.

The second observation is the majority of stress softening occurs during the first stretch. As shown in Figure 3 (a), comparing the first stretch (loading) with the first release (unloading), the stress is lowered substantially. During the second and third cycles, there is still stress softening. However, the level of softening is marginal. We use the area enclosed the loading and unloading curves, which characterizes the dissipated energy density (energy loss per unit volume), to quantify the stress softening. The dissipated energy density (dissipated energy/volume) during the first cycle registers at 4.32 $\mathrm{J/cm^3}$, in sharp contrast with 1.41 $\mathrm{J/cm^3}$ and 1.35 $\mathrm{J/cm^3}$ for the second and third cycles separately.

The third observation is the continuous stress softening when the strain exceeds the previous maximum strain ever applied. As shown in figure 3(b), three loading-unloading cycles are applied, and the applied strain increases from 100%, 200%, to 300%. As a reference, an independent monotonous stretch (loading only) with strain up to 300% is conducted and its stress-strain curve is also plotted in figure 3(b). It can be seen that the stress-strain curve almost returns to the reference curve once the strain exceeds the previous strain, and stress softening, which diminished after the first stretch, arises again.

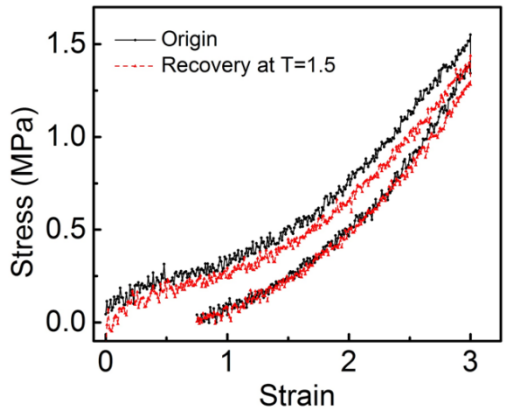

Figure 4 Recovery of the Mullins effect when exposed to elevated temperatures.

The fourth observation is the recovery of the Mullins effect at elevated temperatures. Both permanent set and stress softening can be fully recovered when exposed to elevated temperature for a long time, which has been verified by various experiments [1,15,41]. It is worth mentioning that even at room temperature, a partial recovery of stress softening and residue strain is possible if the relaxation time is long enough. For instance, Rigbi observed a partial stress recovery of a carbon-black filled rubber given a four-week relaxation without temperature change [42]. The temperature and time dependence indicates the underlying mechanism of the Mullins effect is a reversible rate process. In our simulation, a similar recovery enabled by temperature is also observed. The original loading and unloading simulation is conducted at T*=1. Without further treatment, the permanent set as well as stress softening will be preserved in the stretched rubber. However, if the stretched rubber is exposed to higher temperature ($T^* = 1.5$) under NVT ensemble for 8 x 10^5 time steps (4.9 ns physical time), the Mullins effect recovers. As shown in figure 4, the black solid curve is from the virgin stretched one, and the red dashed curve is the stress-strain curve measured after the stretched rubber exposed to elevated temperature. We can see that the stress softening appears in the recovered rubber.

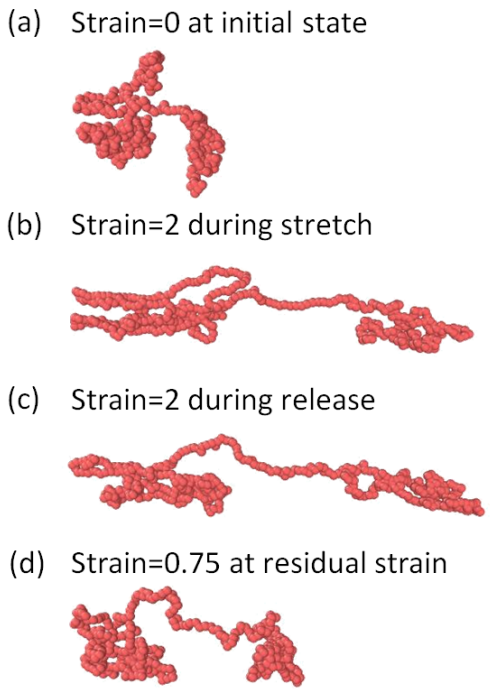

Figure 5 A representative elastomer chain at different strains. The maximum strain is 3.

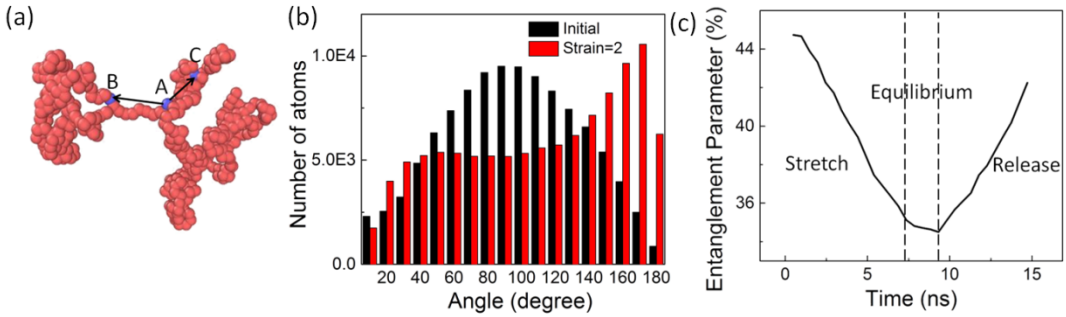

Figure 6 Characterization of chain entanglement. (a). Illustration of a flexion node. (b) Atom number as a function of angle at two states (strain = 0 and 2). (c) The change of entanglement parameter in a stretch-release process.

Resting on the consistent regeneration of key characteristics of the Mullins effect using MD simulation, it is time to gain insight into microstructure changes. We first look at the chain movement of a representative elastomer. Its structure at different strains is plotted in Figure 5. We can clearly see the folding and unfolding process is in accordance with stretching and releasing. We use a method developed by Yashiro et al [43] to quantify the chain entanglement. The detail of the method is described as follows. Starting from a target node (monomer), two vectors are drawn by pointing to the 10th forward/back monomers as shown in Figure 6(a). The angle formed between the two vectors is used to evaluate the type of the node. The node is viewed as a flexion node if the angle is smaller than the pre-defined critical angle (90°), otherwise it is called a normal node. Following Yashiro's work, Hossain et al [28] further define the entanglement parameter as the total fraction of flexion nodes to quantify the system entanglement. We adopt the same method to track the entanglement evolution in our simulation. Figure 6(b) presents the distribution of atom

as a function of angle at initial and stretched state (strain = 2). When there is no external strain, as we expected, the distribution of node angle exhibits a near Gaussian distribution with the mean angle of 90°. When the strain increases to 2, the amount of polymer monomers with large node angle increases, and the entanglement parameter is thus decreased accordingly. To show the dynamic evolution, the entanglement parameter is calculated as a function of time in a stretch-release process as shown in Figure 6(c). The entanglement parameter decreases monotonically with the increase of tensile strain. At the end of stretching, the NVT equilibrium is performed. As we can see, the entanglement parameter will continue to decrease during the equilibrium. Upon releasing the entanglement parameter increases. However, it cannot recover to its original state. The unrecovered entanglement is correlated with the property change, stress softening and permanent set.

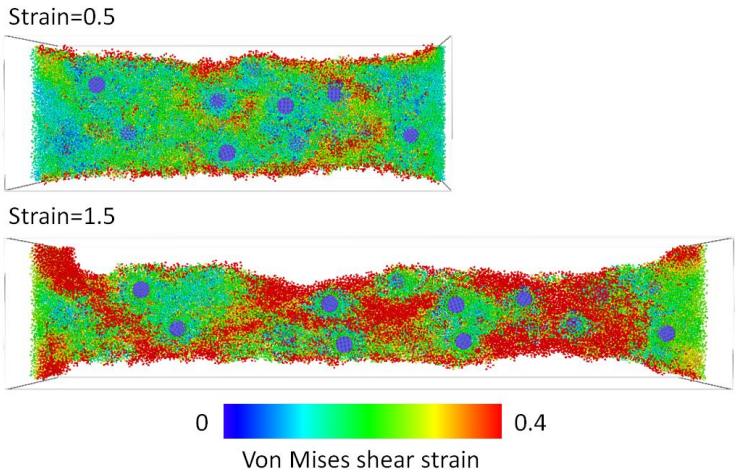

Figure 7 Internal deformation map of filled rubber at two strains (0.5 and 1).

Up to point, we have examined the microstructure change of polymer matrix and identified that it strongly correlates with the Mullins effect. The next question is what happened at the filler/polymer interface? We then map the microstructure change of the whole system using internal atomic von Mises shear strain. To reflect the internal, microscopic shear strain of atoms, the homogeneous cell strain resulting from stretching is removed. In this way, the atomic strain obtained is the reflection of deviation from the average strain, which is a better indicator for microstructure change. The sliced images colored based on atomic shear strain are presented in Figure 7 at two macroscopic strains (0.5 and 1.5)**.** It is interesting to see that the system is clearly divided into three regimes in term of atomic strain. For fillers, there is no internal deformation because they are treated as rigid. This is also true in reality because fillers have much higher mechanical yield strength. For polymer matrix, as reflected in our previous entanglement analysis, there is severe excess strain. In between filler and polymer matrix, an interfacial regime with intermediate strain arises. Tt is revealed that the deformation is strongly heterogeneous. Excess deformation occurs in polymer matrix. The heterogeneous microstructure change revealed by MD simulation has broad implication for the development of fatigue models for rubber. It is noted that Akutagawa et al made attempts to include the realistic filler cluster structure obtained from experimental characterization (in contrast to ideal filler distribution) into finite element analysis (FEA), a surprisingly high excess strain on the level of 200% was observed even if the macroscopic strain is only 15% [44]. Our simulation confirms the existence of heterogeneous plastic deformation. However, the quantitative agreement cannot be achieved. The MD result shows 40% excess strain for a 50% macroscopic strain. We attribute the quantitative discrepancy to the continuum assumption used in FEA. The continuum assumption cannot tell the microstructure

difference between different regimes, whereas MD simulation is able to capture the difference of atomic structure and dynamics and thus is more reliable. The inability of considering the microstructure difference may give rise to issues when extending FEM to fracture and fatigue models. The microstructure heterogeneity is essential for the occurrence of fracture and fatigue. Most of the current available fatigue and fracture models are, however, based on continuum variables, to which the micro level heterogeneity is averaged out [45–48]. The knowledge of material structure heterogeneity provides in-depth microstructure information for the development of new fracture and fatigue models for rubber materials.

Discussion and conclusion

As we have demonstrated, MD simulation is able to capture the four key characteristics of the Mullins effect, and the further microstructure analysis reveals that the disentanglement of polymer chain is responsible for the Mullins effect. Before stretching, polymer chains arrange themselves in a packing state. If we divide an elastomer chain as multiple segments, some segments overlap with each other, which only gives rise to a very small barrier for the relative motion, and some segments entangle with each other (from either the same chain or different chains), which can significantly reduce the mobility of these segments. When subjected to the first stretch, the overlapped segments will be firstly aligned along the stretching direction because of the smaller barrier, whereas the entangled segments require much larger external stress. Reflected in the stress-stain curve, it is a stress enhancement. Upon releasing, the overlapping state can be easily recovered. However, the entanglement state cannot be fully recovered due to the larger barrier. The inability to recover all entanglements of chain segments leads to the stress softening and residual strain.

The Mullins effect is actually not permanent. The argument that the disentanglement is irreversible is pre-conditioned by under the same temperature. The Mullins effect, or chain disentanglement in molecular level, can be partially recovered when raising the system to a higher temperature for a long time, enabling polymer chains with sufficient mobility (temperature) and possibility (time) to gain more entanglements. This full recovery can only occur when the disentanglement is to overcome physical interaction, instead of chemical bonding. The formation of chemical bond is extremely difficult considering its requirement for two dangling bonds and much higher temperature. Any molecular interpretation based on chemical bond rupture (polymer/filler bond rupture, chain or crosslink rupture in polymer matrix, and filler cluster bond rupture) is unfavorable in this sense. The proposed interpretation based on disentanglement is also in line with the experimental observation discussed in the introduction section. Swelling tests have shown that there is no significant crosslink or chain breakage after stretching [16,24], which is consistent with our explanation that disentanglement originates from physical interaction.

As revealed by our simulation, the polymer chain disentanglement is physically sufficient to interpret the Mullins effect. We thus further conclude that the Mullins effect can be described by transition state theory. A single disentanglement event is an individual rate process, numerous local disentanglement events driven by external stress collectively cause the macroscopic stretch and associated stress softening. For a single local entanglement or disentanglement, it can be viewed as a transition process between two states separated by energy barriers. The transition rate (from one state i to another state j) can be formulated as $\kappa_{ij} = f\exp\left(-\frac{\Delta E_{ij}}{k_B T}\right)$ [49]. f is the attempt frequency of the transition, ΔE_{ij} is the energy barrier from i to j, k_B is the Boltzmann constant, and T is temperature. Based on the equation, the effect of temperature on disentanglement is explicit. As a stress-driving rate process, stress is able to alter the energy landscape. The effect of stress on the energy barrier can be linear or sub-linear depending on the shape of the energy landscape [50]. Although time has no influence on transition rate, it does influence the occurrence of transition. Given a transition rate, time will increase the possibility for the the occurrence of transition. Compared with temperature and stress, the effect of time on disentanglement however is much weaker, on

the logarithmic scale. This is consistent with experimental observations, in which time, stress and temperature all can affect the Mullins effect, but time is a second order factor compared with stress and temperature. This molecular insight and the possibility to apply transition rate theory lay out a theoretical framework to formulate constitutive equations for filled rubber taking account of microscopic dynamics.

There is, indeed, one experimental observation not captured by our simulation. Comparing Figure 1 with Figure 3, the stress softening in experiment progressively increases with strain whereas the stress softening in our simulation increases moderately. We attribute the discrepancy to the model simplification. Our simulation, a CG MD model, cannot take account of all aspects of a silica-filled SBR system. Firstly, spherical fillers are ideally dispersed in polymer matrix and there is no reversible agglomeration and irreversible aggregation. The experimental observation that there is no direct correlation between the Mullins effect and filler cluster rupture registered by electrical conductivity measurement [16] does exclude the irreversible filler aggregation; however, it cannot rule out the filler agglomeration as possible mechanism. We believe the filler agglomeration resulted from physical interaction may contribute to the stress softening, bridging the gap between our simulation and experiment. Secondly, the spring-bead model for elastomer simplifies a monomer with geometrical complexity as a spherical bead, as a result, the physical entanglement caused by geometrical complexity is neglected in simulation. If equipped with a full atomistic model, the extra entanglement would contribute significantly to stress softening, further bridging the gap.

In summary, we have developed a CG molecular dynamics model to study the Mullins effect. For the first time, four key characteristics associated with the Mullins effect are re-produced. The microstructure analysis revealed that the polymer chain entanglement and disentanglement are concomitant with stress increase and decrease. The disentanglement is not completely reversible after the first stretch, and the irreversible disenchantment is responsible for permanent set and stress softening. Because entanglement stems from physical interaction, the full recovery of the Mullins effect is realized when exposed to elevated temperature. The ability to have a full recovery of the Mullins effect also eclipses the possible explanations based on chemical bond rupture, including chain and crosslink breakage, filler/polymer bond rupture, filler cluster bond rupture. On the other hand, due to the limitation of our simulation, we cannot exclude the contribution from filler agglomeration, which has a physical interaction origin (physical interaction between filler/filler and filler/polymer) as well. We also anticipate that the full atomistic model of monomer structure may give rise to larger stress softening than that predicted in the current coarse grained model. Finally, when subjected to stretch, a strong heterogeneous deformation map, clearly divided into three distinct regimes, is demonstrated, shedding light on the formulation of continuum fatigue model for filled rubber.

Acknowledgement

The authors would like to acknowledge the NSF Center for Tire Research (CenTiRe) for its financial support. We also thank Kejing Li and Jim Palombo for their constructive suggestions. This work was supported in part by an allocation of computing time from the Ohio Supercomputer Center.

Reference

[1] Harwood J A C and Payne A R 1966 Stress softening in natural rubber vulcanizates. Part III. Carbon black-filled vulcanizates *J. Appl. Polym. Sci.* **10** 315–24

[2] Harwood J A C, Mullins L and Payne A R 1965 Stress softening in natural rubber vulcanizates. Part II. Stress softening effects in pure gum and filler loaded rubbers *J. Appl. Polym. Sci.* **9** 3011–21

[3] Hanson D E, Hawley M, Houlton R, Chitanvis K, Rae P, Orler E B and Wrobleski D A 2005 Stress

softening experiments in silica-filled polydimethylsiloxane provide insight into a mechanism for the Mullins effect *Polymer (Guildf).* **46** 10989–95

[4] Litvinov V M, Orza R a, Kl M, Duin M Van and Magusin P C M M 2011 Rubber À Filler Interactions and Network Structure in Relation to Stress À Strain Behavior of Vulcanized , Carbon Black Filled EPDM *Macromolecules* **44** 4887–900

[5] Luo H, Klüppel M and Schneider H 2004 Study of filled SBR elastomers using NMR and mechanical measurements *Macromolecules* **37** 8000–9

[6] Mullins L 1969 Softening of Rubber by Deformation *Rubber Chem. Technol.* **42** 339–62

[7] Hirotsu S 1991 Softening of bulk modulus and negative Poisson's ratio near the volume phase transition of polymer gels *J. Chem. Phys.* **94** 3949

[8] and R E W, Creton* C, Brown H R and Gong J P 2007 Large Strain Hysteresis and Mullins Effect of Tough Double-Network Hydrogels *Macromolecules* **40** 2919–27

[9] Storm C, Pastore J J, MacKintosh F C, Lubensky T C and Janmey P A 2005 Nonlinear elasticity in biological gels *Nature* **435** 191–4

[10] Chaudhuri O, Parekh S H and Fletcher D A 2007 Reversible stress softening of actin networks *Nature* **445** 295–8

[11] Mullins L and Tobin N R 1965 Stress softening in rubber vulcanizates. Part I. Use of a strain amplification factor to describe the elastic behavior of filler-reinforced vulcanized rubber *J. Appl. Polym. Sci.* **9** 2993–3009

[12] Bouasse H and Carrière Z 1903 Courbes de traction du caoutchouc vulcanisé *Ann. la Fac. des Sci. Toulouse* **5** 257–83

[13] Mullins L 1948 *Effect of Stretching on the Properties of Rubber* vol 21

[14] Heinrich G, Klüppel M and Vilgis T A 2002 Reinforcement of elastomers *Curr. Opin. Solid State Mater. Sci.* **6** 195–203

[15] Diani J, Fayolle B and Gilormini P 2009 A review on the Mullins effect *Eur. Polym. J.* **45** 601–12

[16] Diaz R, Diani J and Gilormini P 2014 Physical interpretation of the Mullins softening in a carbon-black filled SBR *Polymer (Guildf).* **55** 4942–7

[17] Beda T 2007 Modeling hyperelastic behavior of rubber: A novel invariant-based and a review of constitutive models *J. Polym. Sci. Part B Polym. Phys.* **45** 1713–32

[18] Bergström J S and Boyce M C 1998 Constitutive modeling of the large strain time-dependent behavior of elastomers *J. Mech. Phys. Solids* **46** 931–54

[19] Boyce M C and Arruda E M 2000 Constitutive Models of Rubber Elasticity: A Review *Rubber Chem. Technol.* **73** 504–23

[20] Charlton D J, Yang J and Teh K K 1994 A Review of Methods to Characterize Rubber Elastic Behavior for Use in Finite Element Analysis *Rubber Chem. Technol.* **67** 481–503

[21] Horgan C O, Ogden R W and Saccomandi G 2004 A theory of stress softening of elastomers based on finite chain extensibility *Proc. R. Soc. London A Math. Phys. Eng. Sci.* **460**

[22] Klüppel M and Schramm J 2000 A generalized tube model of rubber elasticity and stress softening of filler reinforced elastomer systems *Macromol. Theory Simulations* **9** 742–54

[23] Simo J C 1987 On a fully three-dimensional finite-strain viscoelastic damage model: Formulation and computational aspects *Comput. Methods Appl. Mech. Eng.* **60** 153–73

[24] Dannenberg E M and Brennan J J 1966 Strain Energy as a Criterion for Stress Softening in Carbon-Black-Filled Vulcanizates *Rubber Chem. Technol.* **39** 597–608

[25] Li C and Strachan A 2011 Molecular dynamics predictions of thermal and mechanical properties of thermoset polymer EPON862/DETDA *Polymer (Guildf).* **52** 2920–8

[26] Lyulin A V, Vorselaars B, Mazo M A, Balabaev N K and Michels M A J 2005 Strain softening and hardening of amorphous polymers: Atomistic simulation of bulk mechanics and local dynamics *Europhys. Lett.* **71** 618–24

[27] Li C, Jaramillo E and Strachan A 2013 Purdue e-Pubs Molecular dynamics simulations on cyclic deformation of an epoxy thermoset Molecular dynamics simulations on cyclic deformation of an epoxy thermoset *Polymer (Guildf).* **54** 881–90

[28] Hossain D, Tschopp M A, Ward D K, Bouvard J L, Wang P and Horstemeyer M F 2010 Molecular dynamics simulations of deformation mechanisms of amorphous polyethylene *Polymer (Guildf).* **51** 6071–83

[29] Smith G D, Bedrov D, Li L and Byutner O 2002 A molecular dynamics simulation study of the viscoelastic properties of polymer nanocomposites *J. Chem. Phys.* **117** 9478–90

[30] Adnan A, Sun C T and Mahfuz H 2007 A molecular dynamics simulation study to investigate the effect of filler size on elastic properties of polymer nanocomposites *Compos. Sci. Technol.* **67** 348–56

[31] Ghanbari A, Ndoro T V M, Rahimi M, Bo M C and Mu F 2012 Interphase Structure in Silica − Polystyrene Nanocomposites : A Coarse-Grained Molecular Dynamics Study *Macromolecules* **45** 572–84

[32] Liu J, Wu S, Zhang L, Wang W and Cao D 2011 Molecular dynamics simulation for insight into microscopic mechanism of polymer reinforcement. *Phys. Chem. Chem. Phys.* **13** 518–29

[33] Gao Y, Liu J, Shen J, Cao D and Zhang L 2014 Molecular dynamics simulation of the rupture mechanism in nanorod filled polymer nanocomposites. *Phys. Chem. Chem. Phys.* **16** 18483–92

[34] Gao Y, Liu J, Shen J, Zhang L, Guo Z and Cao D 2014 Uniaxial deformation of nanorod filled polymer nanocomposites: a coarse-grained molecular dynamics simulation. *Phys. Chem. Chem. Phys.* **16** 16039–48

[35] Müller-Plathe F 2002 Coarse-graining in polymer simulation: From the atomistic to the mesoscopic scale and back *ChemPhysChem* **3** 754–69

[36] Chi Ma, Tuo Ji, Christopher G. Robertson， R. Rajeshbabu， Jiahua Zhu and Y D Effect of filler/polymer interface on elastic properties of polymer nanocomposites: A molecular dynamics study *Tire Sci. Technol. Accept.*

[37] Mullins L 1949 Permanent Set in Vulcanized Rubber *Rubber Chem. Technol.* **22** 1036–44

[38] Dorfmann A and Ogden R W 2004 A constitutive model for the Mullins effect with permanent set in particle-reinforced rubber *Int. J. Solids Struct.* **41** 1855–78

[39] Yi J, Boyce M C, Lee G F and Balizer E 2006 Large deformation rate-dependent stress–strain behavior of polyurea and polyurethanes *Polymer (Guildf).* **47** 319–29

[40] Andrews R D, Tobolsky A V. and Hanson E E 1946 The Theory of Permanent Set at Elevated Temperatures in Natural and Synthetic Rubber Vulcanizates *J. Appl. Phys.* **17** 352

[41] Laraba-Abbes F, Ienny P and Piques R 2003 A new "Tailor-made" methodology for the mechanical behaviour analysis of rubber-like materials: II. Application to the hyperelastic behaviour characterization of a carbon-black filled natural rubber vulcanizate *Polymer (Guildf).* **44** 821–40

[42] Rigbi Z 1980 Reinforcement of rubber by carbon black *Properties of Polymers* (Berlin, Heidelberg: Springer Berlin Heidelberg) pp 21–68

[43] Yashiro K, Ito T and Tomita Y 2003 Molecular dynamics simulation of deformation behavior in amorphous polymer: Nucleation of chain entanglements and network structure under uniaxial tension *Int. J. Mech. Sci.* **45** 1863–76

[44] Akutagawa K and Nishi T 2013 The nanotech challenge: Creating a nano-architecture design for tire materials development *Tire Technol. Int.*

[45] Mars W V and Fatemi A 2002 A literature survey on fatigue analysis approaches for rubber *Int. J. Fatigue* **24** 949–61

[46] DeSimone A, Marigo J-J and Teresi L 2001 A damage mechanics approach to stress softening and its application to rubber *Eur. J. Mech. - A/Solids* **20** 873–92

[47] Göktepe S and Miehe C 2005 A micro–macro approach to rubber-like materials. Part III: The micro-sphere model of anisotropic Mullins-type damage *J. Mech. Phys. Solids* **53** 2259–83

[48] Govindjee S and Simo J 1991 A micro-mechanically based continuum damage model for carbon black-filled rubbers incorporating Mullins' effect *J. Mech. Phys. Solids* **39** 87–112

[49] Hänggi P, Talkner P and Borkovec M 1990 Reaction-rate theory: fifty years after Kramers *Rev. Mod. Phys.* **62** 251–341

[50] Dong Y, Perez D, Gao H and Martini a 2012 Thermal activation in atomic friction: revisiting the theoretical analysis. *J. Phys. Condens. Matter* **24** 265001